Energy decay of rotating turbulence with confinement effects

C. Morize and F. Moisy[a)]

Fluides, Automatique et Systèmes Thermiques (FAST), Université Pierre et Marie Curie—Paris 6, Université Paris Sud 11, and CNRS (UMR 7608), Bâtiment 502, Campus Universitaire, F-91405 Orsay Cedex, France

The energy decay of grid-generated turbulence in a rotating tank is experimentally investigated by means of particle image velocimetry. For times smaller than the Ekman time scale, a range of approximate self-similar decay is found, in the form $u^2(t) \propto t^{-n}$, with the exponent n decreasing from 2 to values close to 1 as the rotation rate is increased. Even at very weak rotation rates, rotation is shown to have a strong indirect influence on the decay law, by making the integral length scale to quickly saturate to the experiment size through the propagation of inertial waves. The experimental decay exponents are found in good agreement with the predicted values from a phenomenological model based on the exponent of the energy spectrum, in which both the effects of the rotation and the confinement are taken into account. © *2006 American Institute of Physics*.
[DOI: 10.1063/1.2212990]

I. INTRODUCTION

The energy decay of high Reynolds number homogeneous and isotropic turbulence is usually well described by a power law,

$$u^2 = a(t - t^*)^{-n}, \tag{1}$$

where u^2 is the velocity variance, n is the decay exponent, and t^* is a virtual origin.[1–6] Turbulence generated by a grid in wind tunnels has been extensively used to test this law, providing an initial state which is close to homogeneity and isotropy, with the use of Taylor's hypothesis to convert the spatial decay into a temporal decay. The power law starts after a certain time t_0, of order of a few tens of M/V,[4] where M is the grid mesh size and V the fluid velocity. The value of the exponent n depends on whether the size of the energy-containing eddies is free to grow ($n=6/5$) or is bounded by the domain size ($n=2$), with a possible changeover between these two regimes.[6] A self-similar decay can hold as long as the instantaneous Reynolds number remains large enough for the turbulence to remain fully developed. Exponents n in the range 1–1.4 are encountered in the literature for wind-tunnel experiments,[4] a range which is consistent with the value $n=6/5$ predicted by Saffman[3] for unbounded turbulence. This large experimental uncertainty is partly due to the freedom in choosing the virtual origin t^* for determining the exponent n from fit of experimental data.[6]

In the presence of rotation, in addition to the instantaneous turnover time ℓ/u (where ℓ is the characteristic size of the energy-containing eddies), two other time scales are present in the problem, which have opposite effects on the turbulence decay: the rotation time scale, Ω^{-1}, and, for bounded systems, the Ekman time scale, $t_E = h(\nu\Omega)^{-1/2}$, where h is the characteristic size along the rotation axis. The rotation time scale Ω^{-1} is associated to the propagation of inertial waves,[7] which modify the nonlinear energy transfers

and reduce the energy dissipation,[8] an effect which may result in a lower value of the exponent n. On the other hand, the Ekman time scale t_E governs the dissipation of those inertial waves from multiple reflections in the Ekman layers,[9] thus enhancing the energy decay at large time, and shortening the range for a possible self-similar decay even at large Reynolds numbers.

In the experiment of Ibbetson and Tritton,[10] where two grids were suddenly translated in an air-filled rotating annulus, the reduction of the energy decay was hidden by the extra dissipation in the Ekman layers, and could not be observed. On the other hand, in the wind tunnel experiments with a rotating honeycomb of Jacquin *et al.*,[8] a significant range such that $\Omega^{-1} \ll t \ll t_E$ could be achieved, and the expected inhibition of the energy decay has been indeed observed. However, the long-time behavior could not be explored due to the limited extent of the wind tunnel (measurements were restricted to $x/M < 110$, i.e., $t < 110M/V$), and the issue of a possible scaling of the energy decay in the presence of rotation could not be addressed by these authors.

Two candidates for the asymptotic scaling of the energy decay of unbounded rapidly rotating turbulence have been proposed (see, e.g., Ref. 11), which cannot at the moment be discriminated by available experimental or numerical data. First, it may be assumed that the energy transfers are totally inhibited by the rotation, leading to an exponent $n=0$ and a purely viscous decay. This regime may be associated to a k^{-3} spectrum, analogous to the Kraichnan spectrum in the enstrophy cascade regime of strictly two-dimensional (2D) turbulence and, by extension, to the quasigeostrophic spectrum for rotating stratified turbulence.[12,13] On the other hand, based on the assumption that Ω^{-1} is the only relevant time scale for the nonlinear interactions, Squires *et al.*[14] obtained from dimensional analysis a self-similar energy decay with an exponent reduced by a factor of 2 relative to its value in the nonrotating case, i.e., $n=3/5$ according to the Saffman ex-

ponent. Results from large eddy simulations were shown by these authors to compare well with this prediction. This value $n=3/5$ has been also obtained from a $k-\epsilon$ model by Park and Chung,[15] and is also consistent with the eddy-viscosity model from Thangam et al.[16] These models are both based on the k^{-2} spectrum proposed by Zhou[17] for rotating turbulence, which relies on the same assumption of nonlinear interactions governed by Ω^{-1} (see also Ref. 18). Bellet et al.,[19] from numerical integration of an asymptotic quasinormal Markovian closure model, recently obtained a trend consistent with this asymptotic value, with an exponent $n \simeq 0.86$ at the end of the computation.

The aim of the present article is to investigate the combined effects of the background rotation and the confinement in the decay of turbulent kinetic energy in a rotating tank, starting from an approximately homogeneous and isotropic state. The experimental setup, described in detail in Ref. 20, is similar to the one originally proposed by Ibbetson and Tritton.[10] A grid is initially towed through the depth of a rotating water tank, and the turbulence is allowed to decay freely, so that the background rotation gradually affects the entire flow in an homogeneous way. The much larger Reynolds numbers reached in the present experiment compared to that of Ibbetson and Tritton,[10] due to the use of water as the working fluid and larger grid velocities, allow us to give clear evidence of the reduction of the energy decay by the rotation before the dissipation in the Ekman layers becomes dominant. In particular, both a significant self-similar decay regime at early time and an Ekman layer dominated regime at larger times are obtained, these two regimes being only separately observed in the experiments of Jacquin et al.[8] and Ibbetson and Tritton.[10]

The article is organized as follows: After a brief presentation of the experimental setup in Sec. II, the measurements of the energy decay, with and without rotation, are described in Sec. III. In Sec. IV a phenomenological model is presented, in which the effects of the rotation and the confinement are taken into account. The exponent of the decay is derived under the assumption of isotropy, large Reynolds number, and a stationary spectrum, and is compared to the experimental results. Finally, some concluding remarks are offered in Sec. V.

II. EXPERIMENTAL SETUP

The experimental setup is the same as the one in Morize et al.,[20] and is only briefly described here. It consists of a water filled glass tank of square section, $L=35$ cm in side, mounted on a rotating turntable, whose angular velocity Ω has been varied between 0.13 and 4.34 rad s^{-1}. A cover is placed below the free surface at a distance $h=44$ cm from the bottom, so that the volume of working fluid is $hL^2 =54$ l. After the fluid is set in solid body rotation, turbulence is generated by rapidly towing a co-rotating square grid, that consists of square bars of 1 cm with a mesh size of $M =39$ mm and a solidity ratio (solid to total area) of 0.45, at a constant velocity $V_g=0.65$ m s^{-1} from the bottom to the top of the tank. During the decay of turbulence, the grid is kept fixed at the top of the tank. The grid Reynolds number is
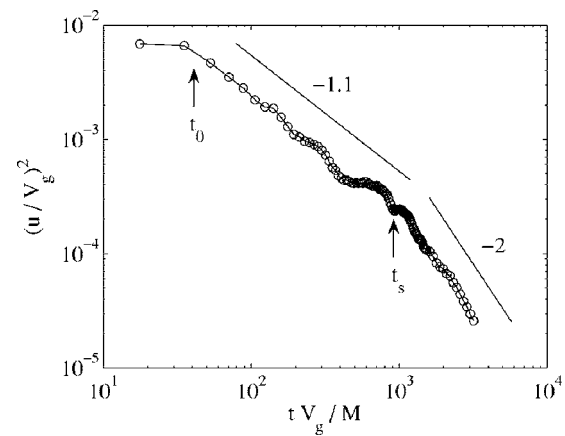
FIG. 1. Energy as a function of time in the absence of rotation. t_s is the time of saturation of the energy-containing length scale.

$Re_g=MV_g/\nu=2.5\times10^4$, a value larger than that of most conventional wind-tunnel experiments, insuring a fully developed turbulence initial state. The grid Rossby number, $Ro_g =V_g/2\Omega M$, is relatively large even for high rotation rate, between 2 and 65, in order to minimize the effect of the rotation on the turbulence production in the wake of the grid.

Instantaneous velocity fields in the horizontal plane at midheight of the tank are obtained from particle image velocimetry (PIV). The flow is illuminated by a horizontal laser sheet, and imaged through the transparent bottom of the tank with a high resolution co-rotating camera. As the root mean square (rms) velocity decreases in time, the delay between the two successive images of a pair is made to gradually increase during the acquisition sequence, from approximately 1 to 100 ms. Interrogation windows of size 16 $\times16$ pixels, with an overlap of 8 pixels, were used for the PIV computations. The final velocity fields are defined on a 160×128 grid, with a resulting spatial resolution of 1 mm.

Each realization of the decay being highly fluctuating, convergence of the statistics is achieved by computing ensemble averages for the same time delay after the grid translation over several independent realizations of the decay. Approximately 50 decays are recorded for each rotating rate Ω, and typically 100 image pairs are acquired during each decay. The horizontal contribution of the turbulent kinetic energy in the plane at midheight,[21]

$$u^2(t) = \langle(u_x - \langle u_x\rangle)^2\rangle + \langle(u_y - \langle u_y\rangle)^2\rangle$$

(where $\langle\rangle$ denotes ensemble and spatial average) is measured as a function of time, with a resolution of 5%. The origin, $t=0$, is taken as the time at which the grid passes through the measurement plane.

III. EXPERIMENTAL MEASUREMENTS OF THE ENERGY DECAY

A. Decay without rotation

For the sake of comparison with the rotating case, the energy decay is shown first for $\Omega=0$ in Fig. 1. An approximate power law is present for $40<tV_g/M<1000$, with an exponent $n\simeq1.1\pm0.1$. Although the Reynolds number is

large, the quality of the power law is modest, with slow oscillations superimposed on the overall decay. Such oscillations probably originate from a large-scale flow favored by the confinement, and are even more visible when plotting the total kinetic energy instead of the turbulent kinetic energy. This large-scale flow is a frequent feature of closed flows (e.g., oscillating grids experiments in confined geometry[22]) but is shown to disappear in the presence of the background rotation.

The lower cutoff for the self-similar decay, $t_0 V_g/M \simeq 40$, is usually interpreted as the time necessary for the grid wakes to merge. The relatively large value observed here compared to that from conventional wind tunnel experiments is probably due to the larger Reynolds number of the present experiment ($\mathrm{Re}_g \simeq 2.5 \times 10^4$). It is however lower than the extrapolated trend deduced from the data reported by Mohamed and LaRue,[4] which gives Re dependence as $t_0 V_g/M \simeq 0.004\mathrm{Re}_g$, yielding $t_0 V_g/M \simeq 100$ in our experiment.

The decay exponent $n \simeq 1.1$ is close to the value $n = 6/5$ derived by Saffman[3] for unbounded turbulence, indicating that for $t V_g/M < 1000$ the integral scale remains smaller than the experiment size. This exponent is also consistent with the range 1–1.4 reported by Mohamed and LaRue,[4] from the compilation of a large number of wind tunnel experiments under different flow configurations, with various data fitting techniques. Plotting the data as a function of $t - t^*$, introducing a virtual origin t^* [see Eq. (1)], does not significantly alter the power law when choosing $|t^* V_g/M| < 40$, with a variation of n less than 20%. The value for t^* being much smaller than the typical decay duration, in the following $t^* = 0$ is taken for simplicity.

Beyond the large time cutoff, $t_s V_g/M \simeq 1000$, a much sharper decay is observed. The Reynolds number being still large at this crossover, $u(t_s)M/\nu \simeq 430$, this second regime is not associated to the final period of decay, but rather to the saturation of the characteristic size of the largest eddies to the experiment size,[6] beyond which a law t^{-2} is expected (see Sec. IV A). Although the range of time is not large enough for an accurate measurement of the exponent beyond this saturation time, the decay in this second regime is indeed compatible with a t^{-2} law for $t > t_s$.

B. Decay with rotation

We now turn to Fig. 2, where the energy decay is shown in the presence of rotation, for rotation rates between 0.13 and 4.34 rad s^{-1}. At the lowest rotation rate, the energy decay strongly differs from the nonrotating case. After a first crossover, at $t_s' V_g/M \simeq 150$ (further discussed in Sec. III C), a well defined power law is found, over more than one decade, with an exponent $n \simeq 2.03 \pm 0.05$ which is significantly larger than the value 1.1 ± 0.1 at $\Omega = 0$. This power law is surprisingly much better defined than that for the nonrotating case. In particular, it has been observed that the curves for the total and the turbulent kinetic energy are very close, within 10%, suggesting that the suspected important large scale flow for $\Omega = 0$, presumably an eddy of diameter comparable to the box size with an horizontal rotation axis, is strongly inhibited when rotation about the vertical axis is present.
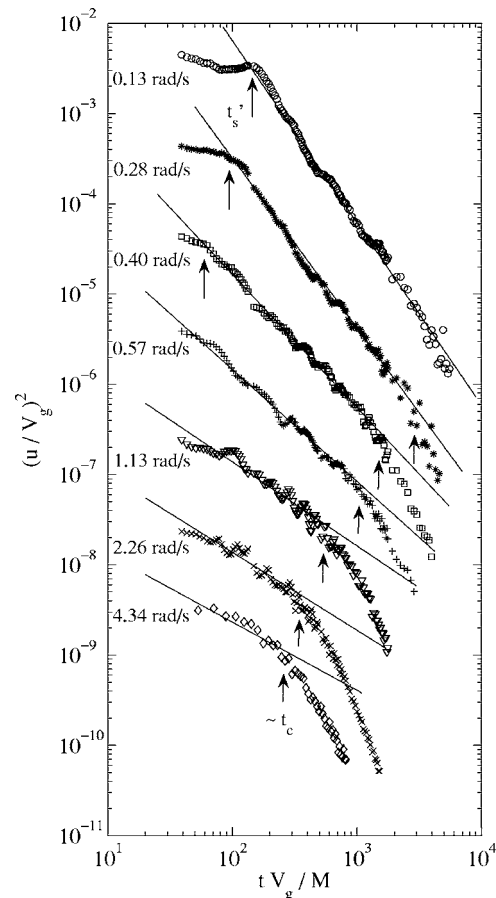
FIG. 2. Energy decay in the presence of rotation for different rotation rates Ω, between 0.13 and 4.34 rad s^{-1}. The upper curve is plotted in the true coordinates, and the following curves are divided by a factor of 10 for visibility. The vertical arrows indicate the rotation-induced saturation time t_s' [Eq. (5)], visible only for the lowest Ω, and the crossover to the Ekman friction dominated regime (not visible for $\Omega = 0.13$ rad s^{-1} due to the limited acquisition time).

As the rotation rate is increased, the rate of energy decay becomes weaker, a clear signature of the reduction of the energy transfer by the background rotation. However, the range of self-similar decay becomes much smaller, and the quality of the power law becomes questionable for Ω larger than 1 rad s^{-1}. Moreover, small oscillations of period $T V_g/M = 2\pi \mathrm{Ro}_g$ (i.e., $T = \pi/\Omega$) superimpose to the decay, originating from inertial waves excited by the grid translation. It is remarkable that these oscillations do not cancel out in the ensemble average, indicating that the phase origin for these waves is indeed fixed by the grid translation.

The rapid falloff of the curves at large time, indicated by the arrows in Fig. 2, is best appreciated when plotted with a linear temporal scale (see Fig. 3). A well defined exponential decay can be seen, a clear signature of the viscous dissipation from the Ekman boundary layers.[7] The characteristic time t_c, obtained by fitting an exponential decay $\exp(-t/t_c)$ at large time, follows the expected scaling for the Ekman time scale $t_E = h(\nu\Omega)^{-1/2}$ over the whole range of Ω (see Fig. 4),

$$t_c \simeq (0.07 \pm 0.02) t_E. \qquad (2)$$

The independence of this time with respect to the grid velocity V_g has been checked for a particular rotation rate (see the filled circles in Fig. 4).
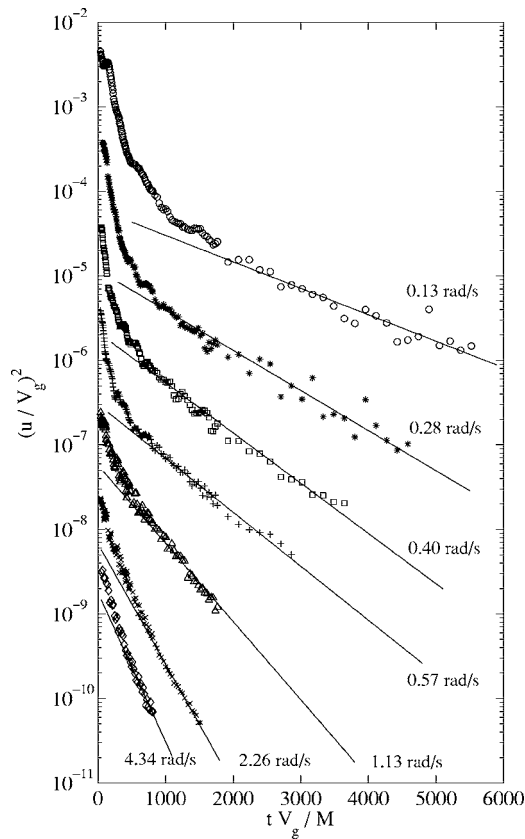
FIG. 3. Same data as in Fig. 2, plotted in linear-logarithmic coordinates. The lines are exponential fits $\sim \exp(-t/t_c)$.

This characteristic time t_c is associated to the dissipation of the inertial waves after multiple reflections over the Ekman layers.[9] It may also be interpreted as the time for the Ekman pumping to damp the vorticity in the eddies, that become preferentially aligned at right angle to the top and bottom walls under the influence of the background rotation.[20,23] In a previous study with the same experiment
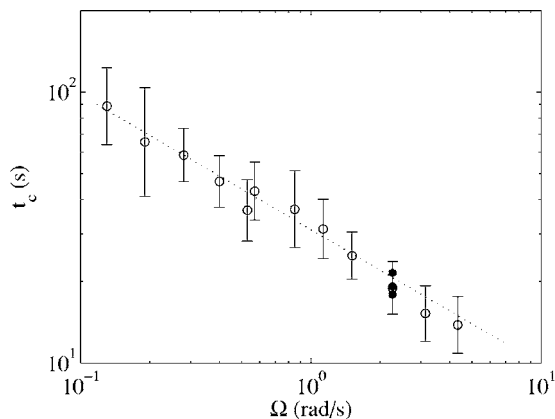
FIG. 4. Time scale of the exponential decay, t_c, as a function of the rotation rate Ω. The grid velocity is $V_g = 0.65$ m s^{-1} ($\bigcirc$), except for $\Omega = 2.26$ rad s^{-1} ($\bullet$), where additional data at different velocities are shown, $V_g \simeq 0.16$, 0.34, and 0.91 m s^{-1}. The line shows a best fit with the Ekman time (2), $t_c \simeq 0.07 h (\nu \Omega)^{-1/2}$.
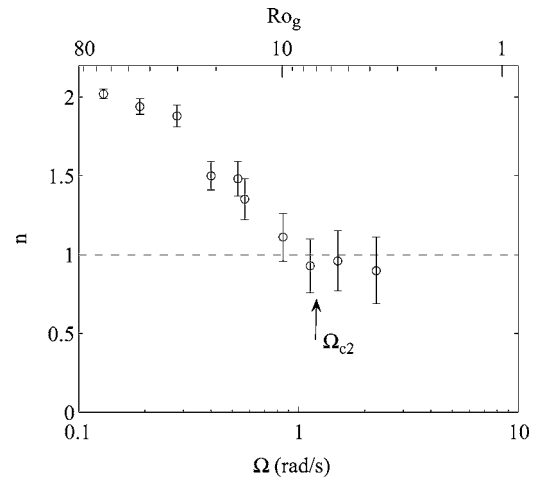
FIG. 5. Decay exponent n as a function of the rotation rate Ω (lower scale) and the grid Rossby number Ro_g (upper scale). The arrow indicates the rotation rate $\Omega_{c2} \simeq 1.3$ rad s^{-1}, above which the rotation-induced saturation time t'_s reaches the time t_0 of the beginning of the power law decay [see Eq. (7)].

(Ref. 20), it has been shown that the skewness factor of the vorticity fluctuations was actually governed by this time scale.[24]

The decay exponent n, obtained by fitting the data in Fig. 2 with two free parameters, a and n [see Eq. (1)] and a virtual origin t^* fixed to 0, is shown in Fig. 5 as a function of the rotation rate. Here again, allowing the virtual origin to be an additional free parameter leads to a variation of n less than 20%, which is comparable to the error bars in Fig. 5 for moderate Ω. The decay exponent decreases continuously from $n \simeq 2$, at $\Omega = 0.13$ rad s^{-1}, to values close to or slightly smaller than 1 for the largest Ω. The large uncertainty for $\Omega > 1$ rad s^{-1} follows from the poor quality of the power laws at large rotation rates, due to the restricted scaling range as Ω is increased. The exponents for such high rotation rates being probably biased by crossover effects, an estimate for n could only be obtained for $\Omega \leqslant 2.26$ rad s^{-1}, and it is not possible to decide from our data whether a saturation toward $n = 1$ (half the value of the weak rotation case) is present or not.

C. Saturation time

The most surprising result of Fig. 5 is that the decay exponent n for the lowest rotation rate, $n \simeq 2$, does not coincide with that for the nonrotating decay, for which $n \simeq 1.1 \pm 0.1$ was observed (see Fig. 1). As shown in the following, this seeming contradiction originates from confinement effects along the rotation axis, which plays a dominant role in the presence of rotation, even for very weak rotation rate.

In the absence of rotation, the energy decay appears to be affected by the confinement after the saturation time $t_s V_g / M \simeq 1000$ (Fig. 1), beyond which the decay was found to be compatible with a t^{-2} law. Assuming an integral scale growing as
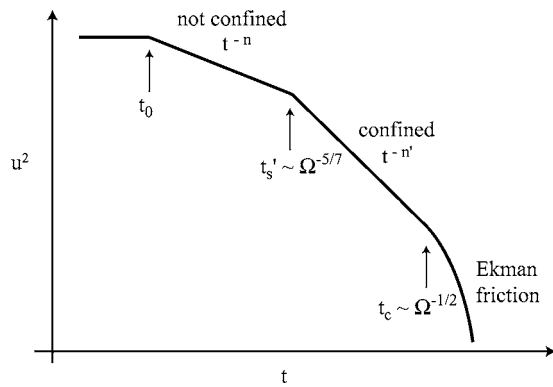
FIG. 6. Sketch of the energy decay in the presence of rotation and axial confinement. The first crossover, t_0, is the time for the grid wakes to merge and produce an approximately isotropic initial state (t_0 is assumed to be independent of Ω, provided that the grid Rossby number Ro_g is large enough). The second crossover, t'_s [Eq. (5)], is the time of saturation of the vertical integral scale induced by the rotation, shown here for $t'_s \gg t_0$, i.e., for $Ro_g \gg Ro_{g,c2}$ [see Eq. (7)], whereas one has $t'_s \simeq t_0$ in the present experiment. The third crossover, t_c, is approximately located at the Ekman time scale [Eq. (2)]. The exponents n and $n' = 5/3n$ corresponds to the nonconfined [see Eq. (13)] and confined [Eq. (15)] regimes, respectively.

$$\frac{\ell(t)}{M} \simeq \alpha \left(\frac{tV_g}{M} \right)^{2/5}, \tag{3}$$

which is a direct consequence of the $t^{-6/5}$ law for the unbounded energy decay (see Refs. 2, 3, and 6 and Sec. IV A), with α a nondimensional factor of the order of unity, this saturation time is given by $\ell(t_s) = L$, i.e.,

$$\frac{t_s V_g}{M} \simeq \left(\frac{L}{\alpha M} \right)^{5/2}, \tag{4}$$

where L is the horizontal size of the tank. The vertical size, h, being slightly larger than L, it will be reached later, providing the turbulence remains isotropic. Using $L/M = 9$ allows us to determine the prefactor, $\alpha \simeq 0.6$.

In the presence of weak rotation, the t^{-2} law begins much earlier (Fig. 2), for $tV_g/M > 150$ instead of 1000, suggesting a much smaller saturation time. This is physically acceptable, as in the presence of rotation the growth of the vertical integral scale is now expected to be governed by inertial waves. Taking $c_g \simeq 2\Omega\ell(t)$ as the group velocity for the fastest inertial waves, with $\ell(t)$ being now the *horizontal* integral scale, the *rotation-induced* saturation time is now defined such that

$$\int_0^{t'_s} 2\Omega\ell(t)dt = h.$$

The growth law for the horizontal integral scale is modified by the rotation, but remains slow, changing from $\ell(t) \propto t^{2/5}$ at $Ro \gg 1$ to $\ell(t) \propto t^{1/5}$ at $Ro \ll 1$ (see Refs. 14 and 18 and Sec. IV B). Keeping the weak rotation law (3), and assuming that $\ell(t)$ remains lower than L (no horizontal saturation at short time), the time for vertical saturation can now be written as[25]

$$\frac{t'_s V_g}{M} \simeq \left(\frac{7}{5} \frac{h}{\alpha M} Ro_g \right)^{5/7}. \tag{5}$$

This time is sketched in Fig. 6. With $h/M = 11.3$, and keeping

the value $\alpha \simeq 0.6$ from the nonrotating case, we obtain $t'_s V_g/M \simeq 200$ for the lowest rotation rate ($Ro_g = 65$), a value indeed much smaller than the saturation time with no rotation, and which is moreover in very good agreement with the Fig. 2 (upper curve). Although this value is larger than the time $t_0 V_g/M \simeq 40$ for the merging of the grid wakes in the absence of rotation (see Fig. 1), above which the turbulence can be considered as approximately homogeneous and isotropic, the range between t_0 and t'_s is probably too small to observe the unbounded decay regime as for the nonrotating case.

It is interesting to note that the Rossby number at which the decay law in the rotating case would actually coincide with that in the nonrotating case may be obtained by equating Eqs. (4) and (5), which yields

$$Ro_{g,c1} = \frac{5}{7} \frac{L}{h} \left(\frac{L}{\alpha M} \right)^{5/2} \simeq 500. \tag{6}$$

This corresponds to a very low rotation rate, $\Omega_{c1} \simeq 0.017$ rad s^{-1} (rotation period of approximately 6 min), a value well below what can be achieved under controlled situation with our rotating turntable. In other words, even for the weakest rotation rate achieved here, the axial confinement plays a significant role from the early time due to the quick saturation of the vertical length scale, and the system quickly enters into a decay regime dominated by the confinement.

At higher rotation rates (Ro_g down to 2), according to Eq. (5), the rotation-induced saturation should occur even faster, with $t'_s V_g/M$ decreasing down to 17, i.e., to values smaller than $t_0 V_g/M$. As a consequence, the system would directly proceed from the initially anisotropic turbulence produced in the wake of the grid to the rotating bounded decay regime, with no intermediate regime of rotating unbounded decay. This picture is however certainly incorrect, as for such large rotation rate the grid turbulence production itself becomes probably affected by the rotation too. From Eq. (5), the minimum Rossby number for which the condition $t'_s > t_0$ remains satisfied is given by

$$Ro_{g,c2} = \frac{5}{7} \frac{\alpha M}{h} \left(\frac{t_0 V_g}{M} \right)^{7/5} \simeq 7, \tag{7}$$

using $t_0 V_g/M \simeq 40$ as for the nonrotating case. This criterion implies $\Omega < \Omega_{c2} \simeq 1.3$ rad s^{-1}, which is indeed satisfied for the present experiment, except for the highest rotation rates (see the two lower curves of Fig. 2). As a consequence, although the grid Rossby number Ro_g is kept larger than unity for all Ω, the highest rotation rates certainly escape from the idealized situation of an homogeneous and isotropic initial state, and the corresponding decay exponents (the last two points of Fig. 5) should be considered with caution.

IV. A PHENOMENOLOGICAL MODEL FOR THE DECAY EXPONENT

In the following, a phenomenological model is introduced to derive the exponent for the decay law in the presence of rotation and confinement, following the approach first used by Comte-Bellot and Corrsin[2] and modified by Saffman[3] for homogeneous turbulence. The procedure con-

sists in linking the decay exponent n to the exponent p of the one-dimensional spectrum, $E(k) \sim k^{-p}$. This approach is motivated by the experimental observation of a steeper spectrum in the presence of rotation,[20] with a spectral exponent p increasing to values slightly larger than 2 at small Rossby number. Both the rotation, by changing the spectral exponent p at large wave number, and the confinement, by introducing a low wave number cutoff, are considered here. However, the anisotropy is not explicitly taken into account at the level of the energy spectrum.

In the following, Sec. IV A briefly recalls the derivation of the decay exponent for nonrotating turbulence, and Sec. IV B extends the procedure using the spectrum modified by the rotation.

A. Decay without rotation

In the absence of rotation, a classical two-range model for the one-dimensional energy spectrum $E(k)$ may be assumed. At small wave number, a "permanent" part

$$E(k) = A k^s \tag{8}$$

holds, where A (of units $m^{s+3} s^{-2}$) is invariant during the decay. In the absence of an external time scale, the decay law is governed by this permanent part,[26] with a decay exponent dimensionally constrained by the value of s, $n = 2(s+1)/(s+3)$. The exponent $s=2$, proposed by Saffman[3] on the basis of momentum conservation, has been found to be consistent with most wind-tunnels experiments,[4,6] and is used in the following. At larger wave number, the Kolmogorov law is used,

$$E(k) = C \epsilon^{2/3} k^{-5/3}, \tag{9}$$

where C is the Kolmogorov constant and ϵ is the instantaneous dissipation rate. The crossover between Eqs. (8) and (9) defines the wave number of the energy-containing eddies, $k_e(t)$, which is a decreasing function of time.

A differential equation for $u^2(t)$ is obtained by equating the energy dissipation rate $-d(u^2)/dt$, where $u^2(t) = \int_0^\infty E(k) dk$ is (twice) the total kinetic energy, and $\epsilon(t)$ in the Kolmogorov spectrum (the Reynolds number is assumed to remain very large during the decay, so that the effect of the viscous cutoff at large wave number can be neglected). If no lower bound for k_e exists (infinite domain), solving for $u^2(t)$ yields the decay law[3]

$$u^2(t) \propto (t + \tilde{t})^{-6/5}, \tag{10}$$

i.e., the decay exponent $n = 6/5$, and the growth law for the integral scale $\ell(t) \simeq k_e(t)^{-1}$,

$$\ell(t) \propto (t + \tilde{t})^{2/5}.$$

In these expressions, the crossover time $\tilde{t} > 0$ does not necessarily correspond to the virtual origin t^* introduced in Eq. (1), even though their order of magnitude should be both given by the time scale of the initial large eddies, $[k_e(0) u(0)]^{-1}$ [with $k_e(0)$ of order of M^{-1} for grid turbulence].

The previous analysis only holds when the energy-containing wave number, $k_e(t)$, remains unbounded during

TABLE I. Summary of the predicted values of the decay exponent n according to the spectral exponent p, with and without confinement. Only the case $s=2$ (Saffman invariant) is considered here for the nonconfined case. Rotating (I) refers to the assumption of energy transfers time scale given by Ω^{-1}, and rotating (II) to the totally inhibited energy transfer regime.

		Decay exponent	
	Spectral exponent	Nonconfined [Eq. (13)]	Confined [Eq. (15)]
Nonrotating	$p=5/3$[a]	$n=6/5$[b]	$n=2$[c]
Rotating (I)	$p=2$[d]	$n=3/5$[e]	$n=1$[f]
Rotating (II)	$p=3$[g]	$n=0$	$n=0$

[a]Kolmogorov.
[b]Reference 3.
[c]Reference 6.
[d]Reference 17.
[e]Reference 14.
[f]Present model.
[g]Kraichnan.

the decay, i.e., if the integral length $\ell(t) \simeq k_e(t)^{-1}$ is allowed to grow without bound. In a physical experiment, where a bounding size L is present, eddies of sizes larger than L cannot exist. This confinement defines a minimum wave number $k_0 \simeq L^{-1}$ toward which $k_e(t)$ will saturate at a given time t_s. A simple way to account for the confinement effect, proposed by Skrbek and Stalp[6] for the nonrotating case, is to take a zero energy density for $k < k_0$. With this description, the energy first decays following approximately the nonconfined law (10) and, for $t > t_s$, solving for $-du^2/dt = \epsilon(t)$ with $k_e(t) = k_0$ now yields the faster decay law

$$u^2(t) \propto (t + \tilde{t})^{-2}.$$

This exponent $n=2$ can be actually recovered in the physical space, by simply assuming that the energy dissipation rate $-d(u^2)/dt$ is u^2/τ, with the dissipation time scale governed by the largest scales, i.e., $\tau = L/u(t)$.

B. Decay with rotation

A crude way to account for the effect of rotation is to modify the exponent p of the high-wave-number part of the spectrum, but without explicitly including the anisotropy in $E(k)$. Although nonphysical, this approach allows us to simply make use of the one-dimensional spectrum $E(k)$, and should therefore apply for moderate Rossby numbers, for which the anisotropy effects remain weak.

Assuming that $E(k)$ depends now on ϵ, Ω, and k, a simple dimensional analysis yields

$$E(k) = C_p \Omega^{(3p-5)/2} \epsilon(t)^{(3-p)/2} k^{-p}, \tag{11}$$

where C_p is a nondimensional constant, that may depend on p. The exponent p is not dimensionally constrained in this expression, and can take any value between 1 and 3. However, the exponent for Ω is expected to be positive, so that p should be restricted to the range 5/3 to 3.

Equation (11) generalizes a variety of situations, summarized in Table I. The Kolmogorov exponent $p=5/3$ is recovered when the limit $\Omega \to 0$ is taken, in order to ensure a nonvanishing spectrum. Similarly, the limit $\epsilon \to 0$ yields

$E(k) = C_3\Omega^2 k^{-3}$, i.e., $p = 3$, which corresponds to the Kraichnan spectrum in the enstrophy cascade regime of strictly 2D turbulence [noted "rotating (II)" in the Table I], with an enstrophy transfer rate taken arbitrarily equal to Ω^3. Finally, the intermediate case $p = 2$, $E(k) = C_2\Omega^{1/2}\epsilon^{1/2}k^{-2}$, is the spectrum proposed by Zhou[17] for rapidly rotating turbulence [noted "rotating (I)" in the Table I], on the assumption of an energy transfer time scale given by Ω^{-1}.

The total kinetic energy $u^2(t) = \int_0^\infty E(k)dk$ can now be computed, using Eq. (8) at small wave number and Eq. (11) at large wave number, and still ignoring the viscous cutoff. A differential equation for $\epsilon(t)$ may be obtained by differentiating $u^2(t)$, but only under the assumption that the exponent p remains constant during the decay. Although not physical (the exponent p being related to the *instantaneous* micro-Rossby number,[20] which decreases during the decay), this strong assumption allows for a simple qualitative connection between p and n. Within this assumption, we obtain, after some algebra (see the Appendix),

$$u^2(t) \propto (t + \tilde{t})^{-n}, \quad \ell(t) \propto (t + \tilde{t})^{n/3}, \tag{12}$$

with

$$n = \frac{3}{5}\left(\frac{3 - p}{p - 1}\right). \tag{13}$$

The asymptotic laws $u^2(t) \propto t^{-6/5}$ and $\ell(t) \propto t^{2/5}$ are recovered for the Kolmogorov spectrum exponent $p = 5/3$, but shallower decay laws are obtained for steeper spectra (see Table I). The k^{-2} spectrum of Zhou[17] yields $u^2(t) \propto t^{-3/5}$ and $\ell(t) \propto t^{1/5}$, i.e., exponents which are twice smaller than the exponents without rotation, as first noticed by Squires *et al.*[14] The limiting case $p = 3$ of the enstrophy cascade regime yields $n = 0$, which is consistent the conservation of energy.

Note that the decay exponent (13) may be generalized for arbitrary values s of the low wave number spectrum [Eq. (8)],

$$n = \frac{s + 1}{s + 3}\left(\frac{3 - p}{p - 1}\right) \tag{14}$$

[and $\ell(t) \propto t^{n/(s+1)}$]. In addition to the Saffman exponent $s = 2$ already considered, the other physically relevant situation is $s = 4$, which is based on the so-called Loistanskii quasi-invariant.[2,5] This value yields slightly larger decay exponents, $n = 10/7$ and $5/7$ for $p = 5/3$ and 2 respectively, with again the factor of 2 between the zero rotation and the fast rotation regimes.

If we finally consider the effect of the confinement, the approach of Skrbek and Stalp[6] may be straightforwardly generalized for the rotating case, taking Eqs. (8) and (11) for the intermediate and large wave numbers and a zero energy density below $k_0 \simeq L^{-1}$. As before, two decay laws are obtained. For $t < t_s'$ (where the saturation time t_s' now depends on Ω), the unbounded decay law modified by the rotation is obtained, with the same exponent (13) as before. For $t > t_s'$, the decay exponent in the rotating and confined regime is now

$$n = \frac{3 - p}{p - 1} \tag{15}$$

[which may be formally obtained by taking $s \to \infty$ in Eq. (14)]. As for the nonrotating case, the exponent with confinement is larger by a factor of 5/3 than that without confinement (see Fig. 6). One now obtains $n = 2$ for $p = 5/3$ and $n = 1$ for $p = 2$, with again the factor of 2 between the zero rotation and the fast rotation regimes. The enstrophy cascade regime ($p = 3$ and $n = 0$) is not modified by the confinement.

C. Comparison with the experiment

The experimental decay exponents n (Fig. 5) are now compared with the values predicted by the model (Table I). The exponents between 2 and 1 found in the experiment are compatible with the possible range of n for $5/3 < p < 2$ when confinement is taken into account [Eq. (15)], confirming the suspected strong influence of the confinement. In Morize *et al.*,[20] the spectral exponent p has indeed been measured from the energy spectrum in the horizontal plane during the decay (see the Fig. 6 of Ref. 20). [The measurement of the exponent s of the low wave number part of the spectrum, Eq. (8), would have required an imaged area much larger than the size of the energy-containing eddies, and has not been carried out.] A gradually increasing exponent p was observed, from $p = 5/3$ for the *instantaneous* micro-Rossby number $Ro_\omega = \omega'/2\,\Omega$ larger than 2 ± 0.5 (where ω' is the vertical vorticity rms) up to values 2.3 ± 0.1 for lower Ro_ω. It is remarkable that, in spite of the unphysical assumption of a spectral exponent p remaining constant during the decay, which is not verified in the experiment, the limiting values at high and low rotation rates compare well with the ones from the model with confinement. In particular, the factor of 2 between these two limiting values predicted by Squires *et al.*,[14] although derived in the absence of confinement, is consistent with the present findings.

The largest values of p reported experimentally, just before the dissipation in the Ekman layers becomes dominant, is $p \simeq 2.3 \pm 0.1$. This value gives $n \simeq 0.54 \pm 0.12$ according to Eq. (15), which significantly underestimates the actual ones ($n \simeq 0.9 \pm 0.2$ for $\Omega \simeq 1$–2 rad s^{-1} in Fig. 5). However, the large uncertainty for n, and the fact that the rotation-induced saturation time t_s' is of the order of t_0 [Eq. (7)], certainly prevent from further comparison between the model and the experiment for such large rotation rate.

It may be tempting to relate the *instantaneous* decay exponent, defined as the local slope $n(t) = -d\ln[u^2(t)]/d\ln t$, to the *instantaneous* spectral exponent $p(t)$, which should yield a relation similar to Eq. (13) or (15) for slowly varying $p(t)$. However, this would lead to a decay exponent decreasing in time, i.e., to a logarithmically convex curve for the energy as a function of time, whereas an approximate power law is obtained experimentally (see Fig. 2). In contrast, such a convex curve is indeed compatible with the rotating wind-tunnel data of Jacquin *et al.*,[8] although over a restricted temporal range, and with numerical data (see, e.g., Ref. 27). It is not clear whether the approximately constant slope of the energy decay in our experiments is a specific feature of the
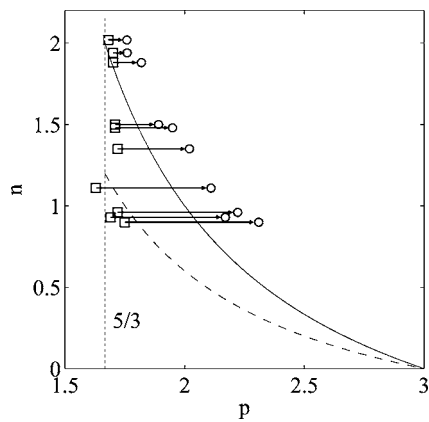
FIG. 7. Decay exponent n as a function of the instantaneous spectral exponent p, for $\Omega = 0.13 - 2.26$ rad s^{-1} (upper to lower arrows). Note that the last two values have $\Omega > \Omega_{c2}$ (see Fig. 5). p measured at the beginning of the power law decay, for $t \simeq \max(t_0, t'_s)$ ($\square$) and p at the end of the power law decay, for $t \simeq t_c$ ($\bigcirc$). The uncertainty on n, not shown here, is given by the error bars in Fig. 5. The curves show the predicted decay exponents: without confinement (13) (– – –) and with confinement (15) (—).

confinement, or an artifact due to the limited available scaling range.

In spite of these uncertainties, more quantitative comparison between the experiment and the model may be provided by plotting the decay exponent n as a function of the instantaneous spectral exponent p (Fig. 7). As p evolves continuously during the decay, only the values at the beginning and the end of the power law range are shown. It is interesting to note that, for all Ω, the starting values for p are still close to the Kolmogorov value, $p \simeq 5/3$, as for homogeneous turbulence, whereas the ending values follow approximately the trend for the decay law exponent with confinement [Eq. (15)]. Although the variation of the spectral exponent is large, the comparison between the data and the two laws [Eqs. (13)–(15)] is clearly in favor of the law with confinement.

V. CONCLUSION

To summarize, clear evidence of the reduction of the energy decay by the rotation has been observed for times smaller than the Ekman time scale. Both a significant self-similar decay at early time and an Ekman layer dominated regime at larger times are obtained, these two regimes being only separately observed in the experiments of Jacquin et al.[8] and Ibbetson and Tritton.[10] The most important result is that, in addition to the dissipation in the Ekman layers, the axial confinement plays a central role in the decay law of rotating turbulence. By making the growth of the integral scale along the rotation axis to quickly saturate to the experiment size even at very low rotation rate, the confinement leads to a sharper decay than for unbounded turbulence, although compatible with the reduced dissipation induced by the rotation. In this second aspect, decaying rotating turbulence in confined geometry strongly differs from that in a wind tunnel with a rotating honeycomb,[8] which may have lateral confinement effects but no confinement along the rotation axis.

When the range between the rotation-induced saturation time of the vertical length scale and the Ekman time scale is large enough, a significant self-similar energy decay is observed, characterized by a decay exponent n decreasing from 2 to values close to 1 as the rotation rate is increased. These exponents are found to be in qualitative agreement with a phenomenological model based on the exponent of the energy spectrum, in which both the effects of the rotation and the confinement are taken into account. The main drawback of this approach is the assumption that the spectral exponent p remains constant during the decay, which is in contradiction with previous experimental observations (Ref. 20). However, it is found that the correlation between the decay exponent and the spectral exponent at large times is in qualitative agreement with model (15) in which the confinement is taken into account. This observation may be of primary importance for the modelling of turbulence in rotating containers, in which the effect of the confinement cannot be neglected even for weak rotation rate and large experiment size.

It is interesting to note that, although the confinement is shown to have a deep influence on the decay of the overall kinetic energy from the early time, other quantities seem to be much less affected by the large scales of the flow. In particular, the spectral exponent and the velocity derivative skewness were shown by Morize et al.[20] to keep their classical (nonrotating) values, $p \simeq 5/3$ and $S \simeq -0.4$, as long that the instantaneous micro-Rossby number Ro$_\omega$ remains large enough. The confinement thus appears to act essentially through the saturation of the integral scale, an effect which is enhanced by the propagation of inertial waves, without much affecting smaller scale quantities, at least for intermediate times. The complex interplay between global quantities, like the grid Rossby number or the Ekman time scale, and more local quantities, like the micro-Rossby number, makes the detailed description of the decay of confined rotating turbulence a rather delicate issue.

APPENDIX: DERIVATION OF EQ. (13)

In the presence of rotation, (twice) the total kinetic energy is obtained by integrating the model spectrum given by Eqs. (8) and (11),

$$u^2(t) = \int_0^{k_e(t)} A k^2 dk + \int_{k_e(t)}^\infty C_p \Omega^{(3p-5)/2} \epsilon(t)^{(3-p)/2} k^{-p} dk.$$

The wave number of the energy-containing eddies follows from the continuity of the two laws at $k = k_e$,

$$k_e(t) = \left(\frac{C_p}{A}\right)^{1/(p+2)} (\Omega^{3p-5} \epsilon^{3-p})^{1/(2p+4)}, \qquad (A1)$$

which gives

$$u^2(t) = \beta_p (\Omega^{3p-5} \epsilon(t)^{3-p})^{3/(2p+4)}, \qquad (A2)$$

introducing the (dimensional) constant

$$\beta_p = \frac{1}{3}\left(\frac{p+2}{p-1}\right) A \left(\frac{C_p}{A}\right)^{3/(p+2)}.$$

The differential equation for $\epsilon(t)$ is obtained by differentiating Eq. (A2). Assuming a stationary spectral exponent p (and hence constant C_p and β_p), one obtains

$$\epsilon = -\frac{3(3-p)}{2p+4}\beta_p \Omega^{[3(3p-5)]/(2p+4)} \epsilon^{-[5(p-1)]/(2p+4)} \frac{d\epsilon}{dt}$$

yielding

$$\frac{d\epsilon}{dt} = -\beta_p^{-1} \frac{2p+4}{3(3-p)} \Omega^{-[3(3p-5)]/(2p+4)} \epsilon^{(7p-1)/(2p+4)}.$$

This differential equation can be readily integrated for $p \neq 1$,

$$\epsilon(t) = \epsilon_0 \left(1 + \frac{t}{\tilde{t}}\right)^{-(2p+4)/[5(p-1)]}, \qquad (A3)$$

where $\epsilon_0 = \epsilon(0)$, and introducing the characteristic time

$$\tilde{t} = \beta_p \frac{3}{5}\left(\frac{3-p}{p-1}\right) (\epsilon_0^{5(1-p)} \Omega^{-3(3p-5)})^{1/(2p+4)}.$$

Integrating (A3) between 0 and t finally yields

$$u^2(t) = u^2(0)\left(1 + \frac{t}{\tilde{t}}\right)^{-(3/5)[(3-p)/(p-1)]},$$

which gives the decay exponent n of Eq. (13). Finally, the growth law for the (horizontal) integral scale is obtained by replacing (A3) in Eq. (A1),

$$\ell(t) = \ell(0)\left(1 + \frac{t}{\tilde{t}}\right)^{(1/5)[(3-p)/(p-1)]}.$$

[1] G. K. Batchelor, *The Theory of Homogeneous Turbulence* (Cambridge University Press, Cambridge, MA, 1960).

[2] G. Comte-Bellot and S. Corrsin, "The use of a contraction to improve the isotropy of grid-generated turbulence," J. Fluid Mech. **65**, 657 (1966).

[3] P. G. Saffman, "Large scale structure of homogeneous turbulence generated at initial instant by distribution of random impulsive forces," J. Fluid Mech. **27**, 581 (1967); "Note on decay of homogeneous turbulence," Phys. Fluids **10**, 1349 (1967).

[4] M. S. Mohamed and J. LaRue, "The decay power law in grid-generated turbulence," J. Fluid Mech. **219**, 195 (1990).

[5] W. K. George, "The decay of homogeneous isotropic turbulence," Phys. Fluids A **4**, 1492 (1992).

[6] L. Skrbek and S. R. Stalp, "On the decay of homogeneous isotropic turbulence," Phys. Fluids **12**, 1997 (2000).

[7] H. Greenspan, *The Theory of Rotating Fluids* (Cambridge University Press, Cambridge, MA, 1968); J. Pedlosky, *Geophysical Fluid Dynamics* (Springer, Berlin, 1987).

[8] L. Jacquin, O. Leuchter, C. Cambon, and J. Mathieu, "Homogeneous turbulence in the presence of rotation," J. Fluid Mech. **220**, 1 (1990).

[9] O. M. Phillips, "Energy transfer in rotating fluids by reflection of inertial waves," Phys. Fluids **6**, 513 (1963).

[10] A. Ibbetson and D. Tritton, "Experiments on turbulence in a rotating fluid," J. Fluid Mech. **68**, 639 (1975).

[11] R. Rubinstein and Y. Zhou, "Schiestel's derivation of the epsilon equation and two-equation modelling of rotating turbulence," Comput. Math. Appl. **46**, 633 (2003).

[12] J. G. Charney, "Geostrophic turbulence," J. Atmos. Sci. **28**, 1087 (1971).

[13] O. Praud, J. Sommeria, and A. Fincham, "Decaying grid turbulence in a rotating stratified fluid," J. Fluid Mech. **547**, 389 (2006).

[14] K. D. Squires, J. R. Chasnov, N. N. Mansour, and C. Cambon, "The asymptotic state of rotating homogeneous turbulence at high Reynolds numbers," Proceedings of the 74th Fluid Dynamics Symposium on Application of Direct and Large Eddy Simulation to Transition and Turbulence, Chania, Greece, AGARD Conf. Proc. **551**, 4-1 (1994).

[15] J. Y. Park and M. K. Chuong, "A model for the decay of rotating homogeneous turbulence," Phys. Fluids **11**, 1544 (1999).

[16] S. Thangam, X.-H. Wang, and Y. Zhou, "Development of a turbulence model based on the energy spectrum for flows involving rotation," Phys. Fluids **11**, 2225 (1999).

[17] Y. Zhou, "A phenomenological treatment of rotating turbulence," Phys. Fluids **7**, 2092 (1995).

[18] V. M. Canuto and M. S. Dubovikov, "Physical regimes and dimensional structure of rotating turbulence," Phys. Rev. Lett. **78**, 666 (1997).

[19] F. Bellet, F. S. Godeferd, J. F. Scott, and C. Cambon, "Wave-turbulence in rapidly rotating flows," J. Fluid Mech. (in press).

[20] C. Morize, F. Moisy, and M. Rabaud, "Decaying grid-generated turbulence in a rotating tank," Phys. Fluids **17**, 095105 (2005).

[21] The velocity variance was misprinted in Ref. 20 [before Eq. (1)], with a wrong factor 1/2.

[22] S. P. McKenna and W. R. McGillis, "Observations of flow repeatability and secondary circulation in an oscillating grid-stirred tank," Phys. Fluids **16**, 3499 (2004).

[23] F. S. Godeferd and L. Lollini, "Direct numerical simulations of turbulence with confinement and rotation," J. Fluid Mech. **393**, 257 (1999).

[24] The slightly lower prefactor for the Ekman time scale obtained here, 0.07 ± 0.02 instead of 0.10 ± 0.02 in Ref. 20 originates from the fitting of the exponential decay, whereas t_c was measured directly as the crossover time from the skewness of the vorticity.

[25] Choosing the rapid rotation law for the growth of the horizontal integral scale, $\ell(t) \propto t^{1/5}$, would not change significantly Eq. (5), with $t_s' \propto \Omega^{-5/6}$ instead of $t_s' \propto \Omega^{-5/7}$.

[26] M. Lesieur *Turbulence in Fluids* (Kluwer Academic, Dordrecht, The Netherlands, 1997).

[27] X. Yang and J. A. Domaradzki, "Large eddy simulations of decaying rotating turbulence," Phys. Fluids **16**, 4088 (2004).